8th International Congress on Civil Engineering,
May 11-13, 2009, Shiraz University, Shiraz, Iran

An error indicator for two-dimensional elasticity problems in the discrete least squares meshless method

Mohammad Naisipour[1], Mohammad Hadi Afshar[1], Behrooz Hassani[2], Majid Zeinali[1]
1- Department of Civil Engineering, University of Science and Technology, Tehran, Iran
2- Department of Civil Engineering, Shahrood University of Technology, Shahrood, Iran

m.naisipour@hotmail.com

Abstract

An error indicator of the discrete least squares method (DLSM) for 2D elastostatic problems is presented. In the DLSM, the problem domain is discretized by distributed field nodes. The field nodes are used to construct the trial functions. The moving least-squares interpolant is employed to construct the trial functions. The least-squares technique is used to obtain the solution of the problem by minimizing the summation of the residuals for the field nodes. The error indicator is readily computed from the residual of the governing differential equation. It is demonstrated, through some elastostatic problems, that the error indicator reflects the exact error.

Keywords: Discrete least squares method, Meshless, Error estimate, Elasticity.

1. INTRODUCTION

Finite element method (FEM) has been successfully used for the simulation of a broad range of applications in the last decades. The method, however, encounters some difficulties when dealing with problems involving moving boundaries, crack propagation or extremely large deformation due to their need for remeshing of the domain. Different methodologies have been suggested by FE practitioners to overcome this problem with varying degrees of success. These methods, however, either partially solve the problem or are computationally very demanding. This has motivated the numerical activists to seek for a method that totally circumvents the mesh generation requirement of the FE and other mesh based methods.

In the last decade a wide range of methods referred to as meshless methods have been devised in an attempt to overcome this problem. These methods are common in that they do not require a mesh with predefined connectivity among the nodes. Some important examples of these methods are the smoothed particle hydrodynamic (SPH) method [1], reproducing kernel particle method (RKPM) [2], element free Galerkin (EFG) method [3], meshless local Petrov–Galerkin (MLPG) method [4] local boundary integral equation (LBIE) method [5], and hp-cloud method [6].

Recently collocation methods are being used more and more to devise meshless methods due to their simplicity and efficiency. These methods, however, lack enough accuracy and more importantly suffer from stability problems when used for non-self adjoint problems. A remedy to this problem has been sought by hybridization of the collocation method with other discretisation schemes mostly least squares method. Arzani and Afshar [7] developed Discrete Least Squares Meshless (DLSM) method for the solution of Poisson equation. While most of the existing meshless methods need background cells for numerical integration, DLSM did not require numerical integration procedure due to the use of least squares method to discretise the governing differential equation. Zhang et al. [8] proposed the Least-squares collocation meshless method to solve elliptic problems. Liu et al. [9] used a Meshless Weighted Least Squares (MWLS) method for the solution of some steady and unsteady heat conduction problems. A sensitivity analysis on the meshless weighted least-square parameters to solve the problems of a cantilever beam and an infinite plate with a central circular hole was performed by Xiaofei et al. [10]. An error estimates for moving least square approximations used for the solution of 1-D convection-diffusion problems was developed by Armentano and Durán [11]. Wang et al. [12] proposed a Point Weighted Least-Squares Meshless (PWLSM) method for the solution of 1-D and 2-D Poisson equations. Firoozjaee and Afshar [13] proposed Collocated Discrete Least Squares Meshless (CDLSM) method to solve elliptic partial differential equations and studied the effect of the collocation points on the convergence and accuracy of the method. The method can be considered as an extension the earlier method of DLSM by introducing a set of collocation points for the calculation of least squares functional. CDLSM was later used by Naisipour et al. [14] to solve elasticity

problems on irregular distribution of nodal points. Afshar and Lashckarbolok [15] used the CDLSM method for the adaptive simulation of hyperbolic problems. A simple posteriori error estimate based on the value of the least squares functional and a node moving strategy was used and tested on 1-D hyperbolic problems. More recently, Afshar et al. [16] examined the effect of the number of collocation points on the accuracy of CDLSM method for both transient and steady state one dimensional hyperbolic problems with uniform nodal spacing.

The purpose of this paper is to describe a simple and efficient error estimator within the framework of the DLSM method. The layout of this paper is as follows: Section 2 provides a brief description of the MLS shape functions used in this work. The DLSM method of discretisation is described in section 3 for a general boundary value differential equation encountered in elasticity problems. The proposed posteriori error estimator is described in section 4. Section 5 illustrates the capabilities of the proposed strategy through some numerical examples, all of them with known analytical solutions. The paper is finally concluded by conclusion remarks in section 6.

2. MOVING LEAST SQUARES SHAPE FUNCTIONS

Among the available meshless approximation schemes, the moving least squares (MLS) method [17] is generally considered to be one of the best methods to interpolate random data with a reasonable accuracy, because of its completeness, robustness and continuity [18,19]. With the MLS interpolation, the unknown function ϕ is approximated by:

$$\phi(X) = \sum_{i=1}^{m} p_i(X)\mathrm{a}_i(X) = P^T(X)\mathrm{a}(X) \tag{1}$$

where $P^T(X)$ is a polynomial basis in the space X coordinates, and m is the total number of the terms in the basis. For a 2D problem we can specify P = [1 x y x2 x y y2] for $m = 6$. a(X) is the vector of coefficients and can be obtained by minimizing a weighted discrete L_2 norm as follows:

$$J = \sum_{i=1}^{n} w_j(X - X_j)\left(P^T(X_j)\, a(X) - u_j^h \right)^2 \tag{2}$$

The weight function $w_j(X - X_j)$ is usually built in such a way that it takes a unit value in the vicinity of the point X_j where the function and its derivatives are to be computed and vanishes outside a region Ω_j surrounding the point X_j . In this research the cubic spline weight function is considered as follows:

$$w(X - X_j) = w(\bar{d}) = \begin{cases} \frac{2}{3} - 4\bar{d}^2 + 4\bar{d}^3 & for\ \bar{d} \le \frac{1}{2} \\ \frac{4}{3} - 4\bar{d} + 4\bar{d}^2 - \frac{4}{3}\bar{d}^3 & for\ \frac{1}{2} < \bar{d} \le 1 \\ 0 & for\ \bar{d} > 1 \end{cases} \tag{3}$$

Where $\bar{d} = \|X - X_j\|/d_w$ and d_w is the size of influence domain of point X_j.
Minimization of equation (2) leads to

$$\phi(X) = P^T(X)A^{-1}(X)B(X)\phi^h \tag{4}$$

where

$$A(X) = \sum_{j=1}^{n} w_j(X - X_j)\, P(X_j)P^T(X_j) \tag{5}$$

$$B(X) = [w_1(X - X_1)P(X_1), w_2(X - X_2)P(X_2), \dots, w_n(X - X_n)P(X_n)] \tag{6}$$

Comparing equation (4) with the well known form of equation (7) yields to equation (8)

$$\phi(X) = N^T(X)\phi^h \tag{7}$$

$$N^T(X) = P^T(X)A^{-1}(X)B(X) \tag{8}$$

$N^T(X)$ contains the shape functions of nodes at point X which are called moving least square (MLS) shape functions and ϕ^h is the vector of nodal parameters.

3. DISCRETE LEAST SQUARE MESHLESS (DLSM) METHOD

Consider the following (partial) differential equation:

$$L(\phi) + f = 0 \qquad in\ \Omega \tag{9}$$

subject to appropriate Dirichlet and Neumann boundary conditions:

$$\phi - \bar{\phi} = 0 \qquad on\ \Gamma_u \tag{10}$$
$$L'(\phi) - \bar{t} = 0 \qquad on\ \Gamma_t \tag{11}$$

where L and L' are (partial) differential operators, f represents external forces or source term on the problem domain, $\bar{\phi}$ is prescribed displacement on the Dirichlet boundary, and $\bar{t}$ prescribed traction on Neumann boundary.

Assume that the problem is discretized using a set of nodal points arbitrarily distributed on the problem domain and its boundaries. Then Eq. (7) can be used to define the residual of governing differential equation at a typical point k which may or may not be a nodal point as:

$$R_\Omega(x_k) = A\big(\phi(x_k)\big) + f(x_k) = \sum_{j=1}^{n} L\left(N_j(x_k)\right)\phi_j + f(x_k) \tag{12}$$

Similarly the residual of Neumann boundary condition at a typical point k on the Neumann boundary can also be written as:

$$R_t(x_k) = L'\big(\phi(x_k)\big) - \bar{t}(x_k) = \sum_{j=1}^{n} L'\left(N_j(x_k)\right)\phi_j - \bar{t}(x_k) \tag{13}$$

and finally the residual of Dirichlet boundary condition at a typical point on the Dirichlet boundary could be stated by:

$$R_u(x_k) = \phi - \bar{\phi}(x_k) = \sum_{j=1}^{n} N_j(x_k)\,\phi_j - \bar{\phi}(x_k) \tag{14}$$

where n is the total number of nodes used to discretize the problem domain and its boundaries. A penalty approach is now used to form the least squares functional of the residuals defined as:

$$I = \sum_{k=1}^{M}\big(R_\Omega^2(x_k)\big) + \alpha_t \sum_{k=1}^{M_t}\big(R_t^2(x_k)\big) + \alpha_u \sum_{k=1}^{M_u}\big(R_u^2(x_k)\big) \qquad ,M = M_d + M_t + M_u \tag{15}$$

where M_d is the number of internal collocation points, M_t is the number of collocation points on the Neumann boundary, M_u is the number of collocation points on the Dirichlet boundary and M is the total number of collocation points. Here α_t and α_u are penalty coefficients for Neuman and Drichlet boundary conditions, respectively. Inserting Eqs (12) to (14) into (15) leads to:

$$I = \sum_{k=1}^{M}\sum_{j=1}^{n}\left[L\left(N_j(x_k)\right)\phi_j + f(x_k)\right]^2 + \alpha_t \sum_{k=1}^{M_t}\sum_{j=1}^{n}\left[L'\left(N_j(x_k)\right)\phi_j + \bar{t}(x_k)\right]^2 + \alpha_u \sum_{k=1}^{M_u}\sum_{j=1}^{n}\left[N_j(x_k)\phi_j + \bar{\phi}(x_k)\right]^2 \tag{16}$$

Minimization of the functional with respect to nodal parameters ($\phi_i, i = 1,2,\dots,n$) leads to the following system of equations:

$$\boldsymbol{K\phi} = \boldsymbol{F} \tag{17}$$

where

$$\boldsymbol{K}_{ij} = \sum_{k=1}^{M} L\big(N_i(x_k)\big)\,L\left(N_j(x_k)\right) + \alpha_t \sum_{k=1}^{M_t} L'\big(N_i(x_k)\big)L'\left(N_j(x_k)\right) + \alpha_u \sum_{k=1}^{M_u} N_i(x_k)N_j(x_k) \tag{18}$$

$$\boldsymbol{F}_i = \sum_{k=1}^{M} L\big(N_i(x_k)\big)f(x_k) + \alpha_t \sum_{k=1}^{M_t} L'\big(N_i(x_k)\big)\bar{t}(x_k) + \alpha_u \sum_{k=1}^{M_u} N_i(x_k)\bar{\phi}(x_k) \tag{19}$$

The stiffness matrix K in Eq. (17) is square (N × N), symmetric and positive-definite irrespective of the characteristics of the differential operators L and L'. Therefore, the final system of equations can be solved via efficient iterative solvers if required.

A note should be made here regarding the value of the penalty parameters. To impose the boundary conditions exactly, the penalty factor must be infinite, which is not possible in practical numerical analysis [20]. Therefore, in the penalty method boundary conditions could not be satisfied exactly, but only approximately. In general, the use of a larger penalty factor will lead to better enforcement of the constraint. On the other hand, if the penalty factor is too small, the constraints will not be properly enforced, but if it is too large, numerical problems will be encountered. A compromise should, therefore, be reached. Penalty coefficients are set to be 10^8 in this work.

4. ERROR ESTIMATE

Adaptivity is an important tool for significantly improving the efficiency of computational methods. Any adaptive procedure is composed of two main components of error estimation and mesh refinement. For any successful adaptive procedure, a reliable error estimator is essential. Different error estimators have been devised and used with different numerical simulation methods and in particular with the FEM. These methods can be divided into two broad classes namely the residual based methods [21, 22 and 22] and the recovery based methods [24 and 25]. In the first method, the residual of the differential equation or some function of the residual is used as a measure of the error. The second approach uses the error in gradient of the solution as the error estimator. These errors are simply calculated by obtaining improved values of gradients using some of the available recovery processes.
In this study, an error estimator based on least squares functional proposed by Afshar and Lashckarbolok [15] for one dimensional hyperbolic problems is adopted. The error indicator used for the nodal refinement is simply defined as:

$$e_k = \sqrt{I(x_k)} \tag{20}$$

where e_k is the value of the error indicator at an arbitrary point on the problem domain or its boundaries, and $I(x_k)$ is the value of the least squares functional, defined by Eq. (15), at point x_k. Since the value of functional represent the extent to which the numerical solution satisfy the governing differential equation and its boundary conditions, the least squares functional defined as the squared residual at an arbitrary point can be considered as a measure of the error of the numerical solution. The proposed error estimator has the advantage of being readily available at the end of each simulation since all the components of the functional are already computed during main simulation. This approach is essentially a point wise approach as it examines errors at individual points. Errors in local and global domains can be evaluated by a simple summation of the point wise errors.

The efficiency and effectiveness of the proposed error estimator is verified in the next section by its application to some benchmark test examples in elasticity.

5. NUMERICAL EXAMPLES

In this section, some 2D numerical examples are solved using the proposed DLSM method and the results error are presented and compared with the exact error obtained from analytical solutions. The examples include: 1) an infinite plate with a circular hole under uniaxial load, and 2) a disc under diametrical compression. Both problems are solved using a second order polynomial basis, m = 6, and a varying radius d_w of the influence domain calculated as proportional to the average distance of six nearest point to the node under consideration.

5.1. INFINITE PLATE WITH A CIRCULAR HOLE

The first example considers the case of an infinite plate with a circular hole subjected to a uniaxial traction *P* at infinity as shown in Figure 1. The exact solutions of this problem can be defined as [26]:

$$\begin{aligned}
\sigma_x &= P\left\{1-\frac{a^2}{r^2}\left[\frac{3}{2}\cos(2\theta)+\cos(4\theta)\right]+\frac{3a^4}{2r^4}\cos(4\theta)\right\}\\
\sigma_y &= -P\left\{\frac{a^2}{r^2}\left[\frac{1}{2}\cos(2\theta)-\cos(4\theta)\right]+\frac{3a^4}{2r^4}\cos(4\theta)\right\}\\
\tau_{xy} &= -P\left\{\frac{a^2}{r^2}\left[\frac{1}{2}\sin(2\theta)+\sin(4\theta)\right]-\frac{3a^4}{2r^4}\sin(4\theta)\right\}
\end{aligned} \tag{21}$$

for the stresses and

$$\begin{aligned}
u_r &= \frac{P}{4G}\left\{r\left[\frac{\kappa-1}{2}+\cos(2\theta)\right]+\frac{a^2}{r}[1+(1+\kappa)\cos(2\theta)]-\frac{a^4}{r^3}\cos(2\theta)\right\}\\
u_\theta &= \frac{P}{4G}\left\{(1-\kappa)\frac{a^2}{r}-r-\frac{a^4}{r^3}\right\}\sin(2\theta)
\end{aligned} \tag{22}$$

for displacements, respectively. Here G is the shear modulus and $\kappa = (3-\nu)/(1+\nu)$ with ν representing the Poisson's ratio.

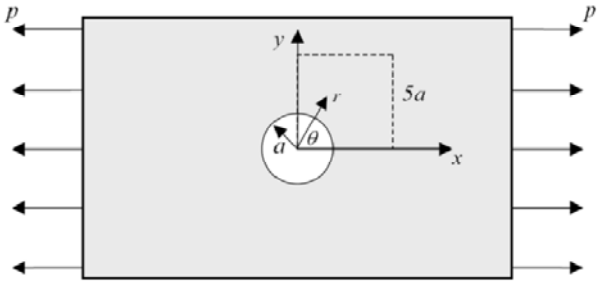

Figure 1. An infinite plate with a circular hole under a uniaxial load P (First example)

Due to symmetry, only the upper right square quadrant of the plate is modeled. The edge length of the square is *5a*, with *a* being the radius of the circular hole. The exact analytical displacements solution is imposed on the left and bottom boundaries and the tractions obtained from the analytical solution [Eq. 21] are applied to the top and right edges. The periphery of the circular hole is traction-free. The problem is solved under a plane stress condition with the following constants: *P*=1, *E*=1000, and *v*=0.3.
The simulation of the problem is performed on an irregular distribution of 197 nodes shown in Figure 2. Figure 3 compares the estimated error and exact error obtained using the following equation:

$$e_i^{exact} = \sqrt{(\boldsymbol{\sigma}_i - \overline{\boldsymbol{\sigma}}_i)^T (\boldsymbol{\sigma}_i - \overline{\boldsymbol{\sigma}}_i)} \qquad (23)$$

where $\boldsymbol{\sigma}_i$ and $\overline{\boldsymbol{\sigma}}_i$ are the exact and approximated stress vectors at node i, respectively.

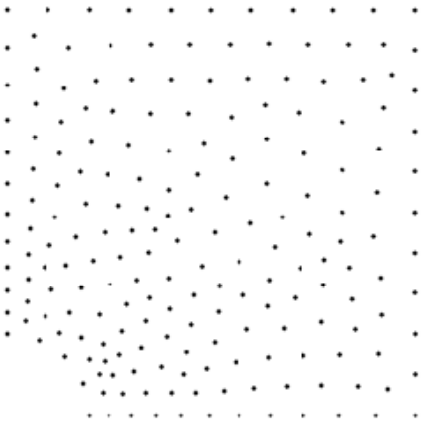

Figure 2. distribution of nodes

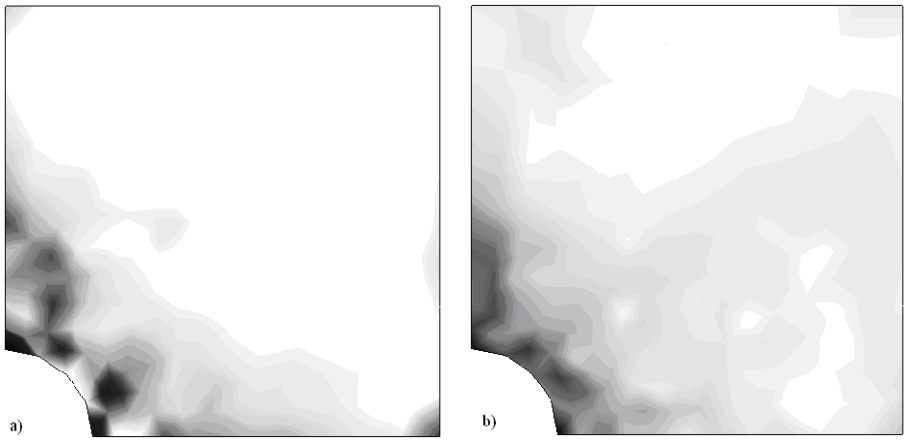

Figure 3. Error distribution on the domain. a: exact error and b: estimated error

5.2. DISC UNDER DIAMETRICAL COMPRESSION

A disc subjected to diametrical compression is considered as the second example as shown in Figure 4.

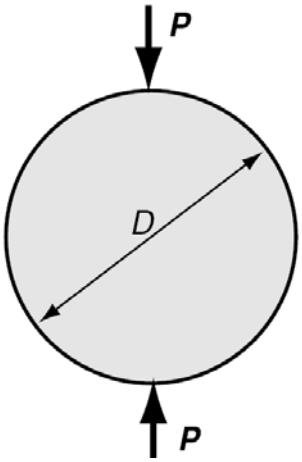

Figure 4. Disc Under Diametrical Compression

For this problem, the exact stress distribution assuming a plane stress condition is given by Saad [27]: as:

$$\sigma_{xx} = -\frac{2P}{\pi}\left[\frac{(R-y)x^2}{r_1^4} + \frac{(R+y)x^2}{r_2^4} - \frac{1}{D}\right]$$
$$\sigma_{yy} = -\frac{2P}{\pi}\left[\frac{(R-y)^3}{r_1^4} + \frac{(R+y)^3}{r_2^4} - \frac{1}{D}\right] \quad (24)$$
$$\sigma_{xx} = \frac{2P}{\pi}\left[\frac{(R-y)^2 x}{r_1^4} - \frac{(R+y)^2 x}{r_2^4}\right]$$

where

$$r_1 = \sqrt{x^2 + (R-y)^2}, \qquad r_2 = \sqrt{x^2 + (R+y)^2} \quad (25)$$

and $R = D/2$ where D is the diameter of the disk. The problem is solved using the DLSM under plane stress condition with the following constants: $P = 1$, $D = 1$, $E = 1$ and $v = 0.3$. The maximum shear stress is calculated using the following expression:

$$\tau_{\max} = \sqrt{\left(\frac{\sigma_x - \sigma_y}{2}\right)^2 + \tau_{xy}^2} \quad (26)$$

A total number of 237 uniformly distributed nodes are used to discretize the problem domain as shown in Figure 5.

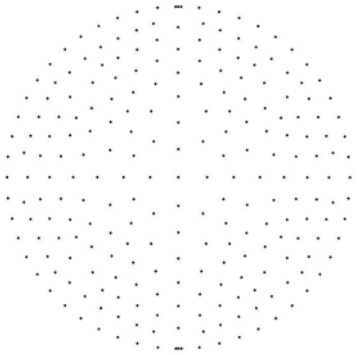

Figure 5. nodal distributions

The counters of exact maximum shearing stress obtained on the initial nodal configuration are plotted in Figure 6. Exact and estimated error distributions the solution error are displayed in Figure 7 showing good agreement despite the relatively coarse initial grid. This indicates on the ability of the proposed error estimator to effectively predict the zones of high numerical errors.

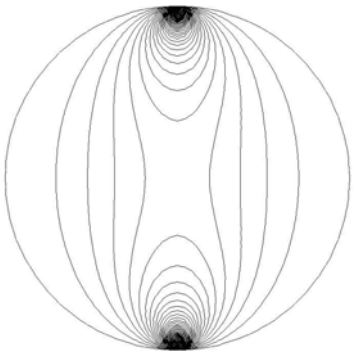

Figure 6. The theoretical maximum shearing stress contours

6. CONCLUSIONS

A *posteriori* error indicator based on least squares functional used to solve the problem was proposed in this paper. It was demonstrated through numerical investigations that the proposed error estimator is able to capture the essential features of exact error distribution. The proposed error estimator has the additional advantage of being readily available at the end of the main analysis and, therefore, requires no extra computational effort for its calculation. The proposed methodology was tested against two benchmark examples from the elasticity and the results were presented and compared to the exact analytical results. The numerical experiments showed capabilities of the proposed methodology to effectively and efficiently estimate the error for solving elasticity problems.

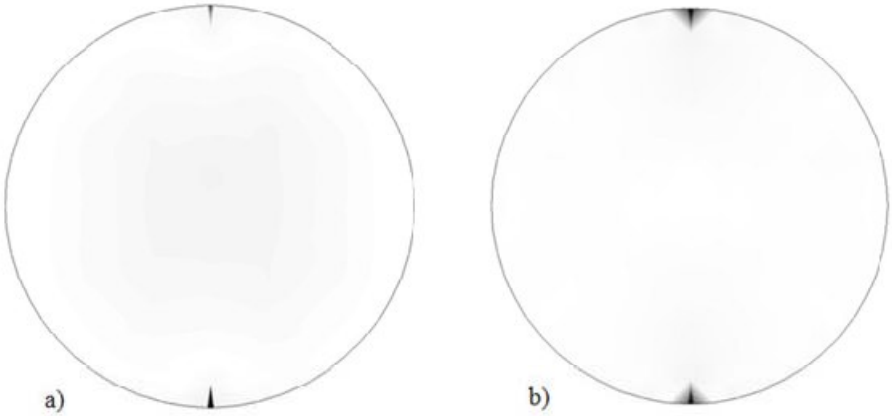

Figure 7. Distribution of error on the nodal distribution. a: Exact error, b: Estimated error

7. REFERENCES

1. Gingold, R. A., Monaghan, J. J., (1977), "Smoothed particle hydrodynamics: theory and applications to non-spherical stars," Monthly Notices of the Royal Astronomical Society, 181:375–389.
2. Liu, W. K., Jun, S., Zhang, Y. F., (1995), "Reproducing kernel particle method," International Journal forNumerical Methods in Fluids, 20:1081–1106.
3. Belytschko, T., Lu, Y. Y., Gu, L., (1994), "Element free Galerkin method," International Journal for Numerical Methods in Engineering, 37:229–256
4. Atluri, S. N., Zhu, T.L., (2000), "The meshless local Petrov–Galerkin (MLPG) approach for solving problems in elasto-statics," Computational Mechanics, 25:169 –179.
5. Atluri, S. N., Sladek, J., (2000), "The local boundary integral equation (LBIE) and it's meshless implementation for linear elasticity," Computational Mechanics, 25:180–198.
6. Liszka, T. J., Duarte, C. A. M., Tworzydlo, W. W., (1996), "hp-meshless cloud method." Computer

Methods in Applied Mechanics and Engineering, 139:263 –288.
7. Arzani, H., and Afshar, M. H., 2006, Solving Poisson's equations by the discrete least square meshless method, WIT Transactions on Modelling and Simulation.42, 23–31.
8. Zhang, X., Liu, X. H., Song, K. Z., Lu, M. W., (2001), "Least-squares collocation meshless method." Int. J. Numer. Meth. Eng., 51:1089–1100.
9. Liu Y, Zhang X, Lu MW., (2005), "A meshless method based on least-squares approach for steady and unsteady-state heat conduction problems," Numerical Heat Transfer, 47(Part B): 257–275.
10. Xiaofei P, Yim SK, Xiong Z., (2004), "An assessment of the meshless weighted least-square method," Acta Mechanica Solida Sinica, 17(3):270-282.
11. Armentano M, Durán R., (2001), "Error estimates for moving least square approximations," Applied Numerical Mathematics, 37:397–416.
12. Wang Q X, Li H, Lam KY., (2005), Development of a new meshless point weighted least-squares (PWLS) method for computational mechanics," Comput Mech., 35:170-181.
13. Firoozjaee, A. R., and Afshar , M. H., (2008), "Discrete least squares meshless method with sampling points for the solution of elliptic partial differential equations," Engineering Analysis with Boundary Elements, in press.
14. Naisipour, M., and Afshar , M. H., Hassani, B., Firoozjaee, A. R., (2008), "Collocation Discrete Least Squares (CDLS) Method for Elasticity Problems and Grid Irregularity Effect Assessment," American Journal of Applied Sciences, 5(11): 1595-1601.
15. Afshar, M. H and Lashckarbolok, M., (2007), "Collocated discrete least square (CDLS) meshless method: error estimate and adaptive refinement," Int. J. Numer. Meth. Fluids, in press.
16. Afshar, MH, Lashkarbolok M, shobeyri G., (2008), "Collocated discrete least squares (CDLSM) method for the solution of transient and steady-state hyperbolic problems," Int. J. Numer. Meth. Fluids, in press.
17. Lancaster, P., and Salkauskas, K., (1981), "Surfaces generated by moving least squares method," Mathematics of computation, 37, 141-158.
18. Onate E., Perazzo, F., Miquel, J., (2001), "A finite point method for elasticity problems," Computers and Structures, 79, 2151-2163.
19. Atluri, S. N., (2004), "The Meshless Local Petrov-Galerkin (MLPG) method for domain & boundary discretizations," Tech Science Press.
20. Liu, G. R.., (2003), "Mesh free methods: moving beyond the finite element method," CRC Press.
21. Babuska, I. and Rheinboldt W. C., (1978), "A posteriori error estimates for the finite element method," International Journal for Numerical Methods in Engineering, 12, 1597 1615.
22. Babuska, I., (1975), "The Self Adaptive Approach in the Finite Element Method," Mathematics of Finite Elements and Applications," (ed. J.R. Whiteman), Academic Press, London, 125-142
23. Babuska, I. and Rheinboldt W.C., (1980), "Reliable Error Estimation and Mesh Adaptation for the Finite Element Method," Computational Methods in Nonlinear Mechanics, (ed. J.T. Oden), 67-108.
24. Zienkiewicz O. C. and Zhu J. Z., (1987), "A simple error estimator and adaptive procedure for practical engineering analysis," International Journal for Numerical Methods in Engineering, 24, 337-357.
25. Zienkiewicz O.C., Zhu J. Z., (1995), "The super convergent patch recovery and a posteriori error estimate. Part 1: The recovery technique," International Journal for Numerical Methods in Engineering, 33:1331–1364.
26. Timoshenko, S. P., and Goodier, J. N., (1987), "Theory of elasticity," 3rd edition, McGraw-Hill, NewYork.
27. Saad M. H., (2005), "Elasticity," Elsevier Butterworth-Heinemann.